

In-plane vibrations of cracked slightly curved beams

H. Rıdvan Öz*

Department of Genetics and Bioengineering, Engineering Faculty, Fatih University,
34500, B.Çekmece, Istanbul, Turkey

(Received October 21, 2009, Accepted August 10, 2010)

Abstract. In-plane vibrations of slightly curved beams having cracks are investigated numerically and experimentally. The curvature of the beam is circular and stays in the plane of vibration. Specimens made of steel with different lengths but with the same radius of curvature are used in the experiments. Cracks are opened using a hand saw having 0.4 mm thickness. Natural frequencies depending on location and depth of the cracks are determined using a Brüel & Kjaer 4366 type accelerometer. Then the beam is assumed as a Rayleigh type slightly curved beam in finite element method (FEM) including bending, extension and rotary inertia. A flexural rigidity equation given in literature for straight beams having a crack is used in the analysis. Frequencies are obtained numerically for different crack locations and depths. Experimental results are presented and compared with the numerical solutions. The natural frequencies are affected too much due to larger moments when the crack is around nodes. The effect can be neglected when it is at the location of maximum displacements. When the crack is close to the clamped end, the decrease in the frequencies in all modes is very high. The consistency of the results and validity of the equations are discussed.

Keywords: curved beam; crack; transverse vibration.

1. Introduction

Curved beams are used in roofs, pipes, gears, electric machinery, pumps and turbines, bridges, reactor vessels i.e., from aeronautics to shipping industry to construction. It is important to understand dynamic behavior of these systems. Vibrations of curved beams with and without crack were investigated by many scientists. Love (1944) presented the equations of motion and their solutions. Ibrahimbegović (1995) considered forced vibrations of a beam with an arbitrary shape. Khan and Pise (1997) studied buried curved piles which was an example of fixed-free boundary condition. Kang and Bert (1997) applied differential quadrature method (DQM) by considering bending moment, radial loading and warping effects. Walsh and White (1999) investigated wave propagation for constant curvature by combining flexure and extensional effects. Tong *et al.* (1998) investigated free and forced vibrations of a circular curved beam assuming inextension of the neutral axis. Krishnan *et al.* (1995) studied free vibrations for different boundary conditions and subtended angles. Chidamparam and Leissa (1995) included extensional effects by considering tangential and normal loadings in pretensioned curved beam. Krishnan and Suresh (1998) calculated

*Corresponding author, Ph.D. Student, E-mail: hroz@fatih.edu.tr

natural frequencies for classical boundary conditions including shear stress and rotary inertia using finite element method (FEM). Exact solutions of free in plane vibrations including extension, shear and rotary inertia were obtained by Tüfekçi and Arpacı (1998). De Rosa and Franciosi (2000) obtained exact and approximate solutions for inextensional case by using another version of DQM. Raveendranath *et al.* (2000) applied FEM by combining polynomial displacement field and considered free vibrations. Oh *et al.* (2000) obtained frequencies and mode shapes for different curves, cross sections and boundary conditions. Özyiğit *et al.* (2004) used FEM (Petyt 1990) to investigate in-plane and out-of-plane vibrations and discussed mode shapes. Some studies included stretching of the neutral axis in transverse vibration, nonlinear behavior and internal resonances (Öz *et al.* 1998, Öz and Özkaya 2005, Öz and Pakdemirli 2006).

Crack propagation is important for fatigue behavior and also for dynamic response of structures. Crack location, type and depth can affect the frequencies and mode shapes. Crack problems in straight beams were investigated widely. Here are some references: Chondros *et al.* (1998) developed continuous crack theory, Kisa *et al.* (1998) combined finite elements and component mode synthesis methods, Fernández-Sáez *et al.* (1999) proposed simple methods for frequencies and calculated approximate frequencies, Bovsunovsky and Matveev (2000) studied dynamic characteristics analytically for a closing crack, Khiem and Lien (2001) calculated frequencies of multiple cracked beam by modeling the cracks as rotary springs using transfer matrix method. Saavedra and Cuitino (2001) presented dynamic behaviors using strain energies given by linear fracture mechanics theory, and Zheng and Kessissoglou (2004) used FEM to calculate natural frequencies and free vibrations. Yang *et al.* (2001) presented, for rectangular cross sectional straight beams, equivalent flexural rigidity for Mode 1 crack case and used in crack identification. There are some studies on the cracked curved beams. Tracy (1975) presented stress intensity factor and Andrasic and Parker (1980) used weight functions, both used mapping-collocation technique to determine the solutions for various geometries and loading conditions. Kapp *et al.* (1980) discussed stress intensity factor for C-shaped specimen. Müller *et al.* (1993) obtained stress intensity factors and strain release rate, and applied to the circular curved beams. Krawczuk and Ostachowicz (1997) calculated natural frequencies of a clamped-clamped arch with an open transverse crack. Nobile (2000) applied strain energy density factor theory (S-theory) to determine crack initiation and direction for straight beams with edge crack. Nobile (2001) studied crack propagation in curved beams using S-theory for mixed mode crack problem and obtained approximate stress intensity factor, and compared with that obtained by Müller *et al.* (1993). Cerri and Ruta (2004) detected localized damage by frequency data of the cracked curved beam. They modeled the crack with a rotary spring attached to both ends and assumed flexural rigidity of the beam was decreasing in the crack zone. Viola and Tornabene (2005) applied generalized differential quadrature techniques to the in-plane free vibrations of thin and thick nonuniform circular arches in undamaged and damaged configurations by modeling an open crack as an elastic hinge with rotational constant. Viola *et al.* (2005) again modeled crack section with an elastic spring and analyzed the problem with an exact analytical method in closed form and differential quadrature method, and presented natural frequencies and mode shapes for different boundary conditions. Alves and Hall (2006) discussed system identification of a concrete arch dam with loss of stiffness in the foundation rock under the action of an earthquake simulation using a finite element model. This was an experimental and numerical study which related decrease in frequencies to loss of stiffness due to cracks. Öz and Daş (2006) used the flexural rigidity equation derived by Yang *et al.* (2001) as an approximation for an open crack in slightly curved beams and presented FEM results for frequencies and mode shapes for

different crack locations and sizes and boundary conditions. Viola *et al.* (2007) studied multi-stepped and multi-damaged arches and modeled cracks with elastic rotational hinges. Cerri *et al.* (2008) performed experiments with cracked curved arches and compared with the results of analytical solutions in which the crack is modeled as a torsional spring. Lotfollahi Yaghin and Hesari (2008) used wavelet analysis to detect a crack in an arch concrete dam.

In this study, the in-plane vibrations of a circular curved beam with a Mode 1 open transverse crack are investigated. In the first section, the results of finite element analysis are presented by Rayleigh beam assumption. In modeling the slightly curved beam, extension of neutral axis, bending, and rotary inertia effects are included. Crack is modeled with a flexural rigidity function. In literature it is mostly modeled as an elastic torsional spring in curved structures. Here flexural rigidity function proposed for straight beams with an open transverse crack given by Yang *et al.* (2001) is used to compare with experimental results. In the experiment, the cracks are made with a hand saw by opening 0.4 mm thick cracks. The beam is freely vibrated after hitting its tip with a hammer and the accelerations are recorded using accelerometers fixed by a magnet, then the spectrums are obtained. The variation of natural frequencies with different crack depths and locations is discussed. Comparisons are made between FEM results and experimental ones. The difference between results is discussed.

2. Finite element method

In Fig. 1, the circular slightly curved beam is shown. The cross section is rectangular; it is a small part of a large circle. Arc length is denoted with L and coordinate is s , R is radius of curvature, γ is elemental arc angle (used in the matrices, see the appendix), EI is flexural rigidity, ρ is volume density and A is the cross sectional area. u and v are tangential and transverse displacements, respectively. The crack location and the depth are c and a , respectively. The crack is at the upper surface and its depth is measured in radial direction. Finite element formulation is given by Özyiğit

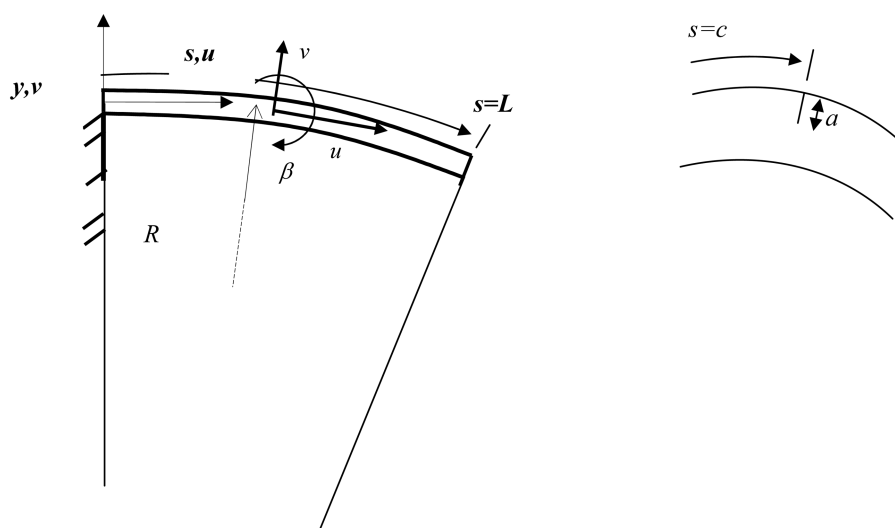


Fig. 1 Clamped free slightly curved beam

et al. (2004) and similar equations can be found in the literature.

The elastic (U) and kinetic (T) energies of the slightly curved Rayleigh beam can be written as follows (Öz and Daş 2006)

$$U = \frac{1}{2}E \int_0^L [A\varepsilon^2 + I\kappa^2] ds, \quad T = \frac{1}{2}\rho \int_0^L [A(\dot{u}^2 + \dot{v}^2) + I\dot{\beta}^2] ds \quad (1)$$

here (\cdot) denotes differentiation with respect to time (t). In-plane strain (ε), curvature change (β), and net cross sectional rotation (κ) in Eq. (1) are defined as follows

$$\varepsilon = \frac{\partial u}{\partial s} + \frac{v}{R}, \quad \beta = \frac{\partial v}{\partial s} - \frac{u}{R}, \quad \kappa = \frac{\partial \beta}{\partial s} = \frac{\partial^2 v}{\partial s^2} - \frac{1}{R} \frac{\partial u}{\partial s} \quad (2)$$

In a straight beam longitudinal and transverse motions are independent in linear vibration assumption. But in curved beams, circumferential and radial motions are dependent and it is expressed by Eq. (2). According to these equations, extensible vibrations are included. In FEM, the following cubic interpolation functions are used.

$$u = a_1 + a_2\xi + a_3\xi^2 + a_4\xi^3 \quad (3)$$

$$v = b_1 + b_2\xi + b_3\xi^2 + b_4\xi^3 \quad (4)$$

where $\xi = s/R\gamma$. Displacement vector for a finite element is

$$[V]_e^T = [u_1 \quad \alpha_1 \quad v_1 \quad \theta_1 \quad u_2 \quad \alpha_2 \quad v_2 \quad \theta_2] \quad (5)$$

where $\alpha = \partial u/\partial s$, $\theta = \partial v/\partial s$. After applying FEM, one can obtain elemental mass and stiffness matrices (see the appendix). Around the crack, the stiffness should decrease. In many articles mentioned in the introduction, the crack is modeled with springs. However an equivalent flexural rigidity for Mode 1 open transverse case in a straight cracked beam for rectangular cross sections ($b \times h$) was presented by (Yang *et al.* 2001) and used by (Öz and Daş 2006) for slightly curved beams in calculating natural frequencies and mode shapes for different end conditions using FEM. Here, the same equivalent flexural rigidity (EI_c) for the cracked beam will be used

$$EI_c = \frac{EI}{1 + \frac{EIR(a,c)}{1 + \left(\frac{(s-c)}{k(a)a}\right)^2}} \quad (6)$$

where

$$R(a,c) = \frac{2D(a)}{k(a)a \left[\arctan\left(\frac{L-c}{k(a)a}\right) + \arctan\left(\frac{c}{k(a)a}\right) \right]}, \quad k(a) = \frac{3\pi(F(a))^2(h-a)^3 a}{(h^3 - (h-a)^3)h}$$

$$D(a) = \frac{18\pi(F(a))^2 a^2}{Ebh^4}, \quad F(a) = 1.12 - 1.4\left(\frac{a}{h}\right) + 7.33\left(\frac{a}{h}\right) - 13.8\left(\frac{a}{h}\right)^3 + 14\left(\frac{a}{h}\right)^4 \quad (7)$$

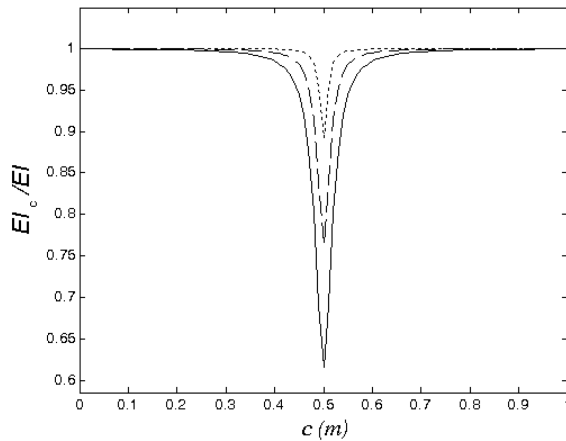


Fig. 2 Variation of the flexural rigidity ratio with the crack location and depth. $a = h/10$ (....), $2h/10$ (---), $3h/10$ (—), the crack location $c = 0.5L$ where arc length $L = 1$ m (Öz and Daş 2006)

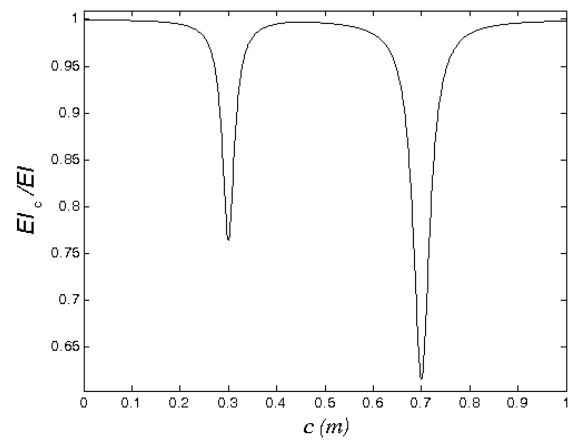


Fig. 3 Variation of the flexural rigidity ratio with the crack locations and depths. $a = 2h/10$ and $3h/10$, the crack location $c = 0.3L$ and $c = 0.7L$ respectively and arc length $L = 1$ m

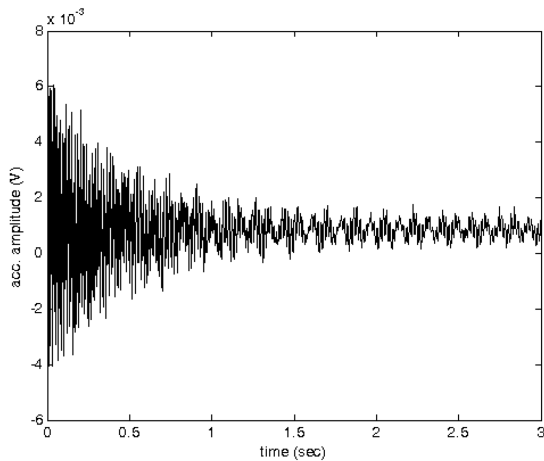
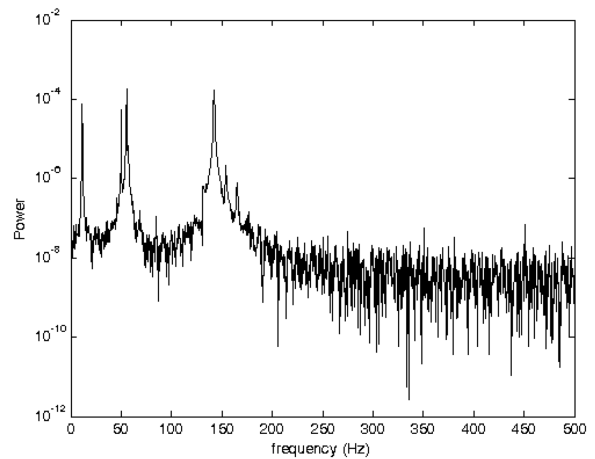
The flexural rigidity Eq. (6) can be inserted into the stiffness matrix and it becomes more effective around crack. Ratio of the flexural rigidity of uncracked beam to that of cracked one is such that it has less effect at points far away from the crack and the effect increases as the point becomes closer to the crack and the flexural rigidity becomes minimum at the crack (Öz and Daş 2006, Yang *et al.* 2001) as shown in Fig. 2 for a single crack for three different crack depths. As the depth becomes larger, the ratio becomes smaller. The ratio approaches to unity away from the crack which is the uncracked case. The numerical solutions are presented in reference (Öz and Daş 2006) for different end conditions. These equations can be used to study multiple cracks with different depths. The Eqs. (6) and (7) are solved for different crack parameters. Variation of the flexural rigidity ratio for two cracks is shown in Fig. 3. It is assumed that the cracks do not affect each other. Experiments are performed for the cracks which are not close to each other.

3. Experimental results and finite element solutions

In this section the experimental setup will be explained and the results will be presented in comparison with the numerical solutions. In the experiment, steel specimens with $E = 207$ GPa and $\rho = 7850$ kg/m³ is used. The specimens have radii of curvature of $R = 1.284$ m and 2.864 m. The members are fixed at one end and the other end is free (clamped-free boundary condition). The specimens are prepared at the workshop. For the specimens having radius of 2.864 m, base $b = 16$ mm, height $h = 2.2$ mm and the lengths are, $L = 0.1, 0.2, 0.3, 0.4$ and 0.5 m respectively. For the specimens having radius of 1.284 m, base $b = 15$ mm, height $h = 2.4$ mm and the lengths are, $L = 0.2, 0.3, 0.4, 0.5, 0.6, 0.7$ and 0.8 m respectively. The setup is shown in Fig. 4. The measurement device is Brüel & Kjaer 4366 type accelerometer located at $c = L/10$ from the support in each test. Voltage calibration coefficient is 4.14 mV/ms⁻². The total weight of the accelerometer, cable and magnet is 89 g. Prosig P5500 device is used to transfer the data to the computer and DATS 4.2.21/2



Fig. 4 Experimental setup

Fig. 5 Acceleration data for no crack case, for $L = 0.4$ m, $R = 2.864$ m, $h = 2.2$ mm, $b = 16$ mmFig. 6 Spectrum for no crack case, for $L = 0.4$ m, $R = 2.864$ m, $h = 2.2$ mm, $b = 16$ mm

software is used in data processing e.g., FFT. The sampling frequency is 1000 Hz and total number of data acquired is 3000.

In the first part of the experiment, the smooth specimens are clamped at one end and the free vibrations are investigated. This case is the uncracked case. In the second part, 0.4 mm wide crack is opened using a hand saw. The experiments are performed for single crack, two cracks and three cracks at different locations. The experimental acceleration and spectrum graphs are given in Figs. 5 and 6 for $L = 0.4$ m, $R = 2.864$ m, $h = 2.2$ mm, $b = 16$ mm for no crack case. The mass of the curved beam is 110.53 gr which is 25% heavier than the measurement system. The natural frequencies measured and numerically calculated are presented in Tables 1 and 2 for different beam samples. The dimensions are given in the tables. Also in the second column of the tables are the weights of the beam specimens. The weight of the measurement system has a decreasing effect on the frequencies. But since the measurement device is attached close to the clamped end, it slightly affects the behavior. In the first mode there is a resemblance between the values obtained

Table 1 The natural frequencies for $R = 2.864$ m, $h = 2.2$ mm, $b = 16$ mm, no crack

L (m)	m (gr)	Method	f_1 (Hz)	f_2 (Hz)	f_3 (Hz)	f_4 (Hz)
0.5	138.16	Test	7.34	41.00	95.00	203.0
		FEM	7.31	45.60	128.0	251.0
0.4	110.53	Test	11.33	55.40	142.0	300.0
		FEM	11.41	71.32	200.0	392.0
0.3	82.90	Test	20.00	85.00	245.5	380.0
		FEM	20.28	126.9	355.6	697.0
0.2	55.26	Test	48.30	194.0	336.5	432.0
		FEM	45.63	286.0	800.0	1568
0.1	27.63	Test	149.0	360.0	402.0	455.0
		FEM	183.0	1143	3197	6257

Table 2 The natural frequencies for $R = 1.284$ m, $h = 2.4$ mm, $b = 15$ mm, no crack

L (m)	m (gr)	Method	f_1 (Hz)	f_2 (Hz)	f_3 (Hz)	f_4 (Hz)
0.8	226.08	Test	2.70	17.40	53.60	96.50
		FEM	3.14	18.69	53.66	106.0
0.7	197.82	Test	3.50	23.00	56.00	121.0
		FEM	4.09	24.64	70.35	138.7
0.6	169.56	Test	4.34	29.70	78.80	150.0
		FEM	5.56	33.82	96.09	189.1
0.5	141.30	Test	6.65	38.50	121.7	225.4
		FEM	7.99	49.06	138.8	272.8
0.4	113.04	Test	10.70	51.50	193.0	330.0
		FEM	12.47	77.12	217.4	427.0
0.3	84.78	Test	20.20	86.30	150.0	261.4
		FEM	22.15	137.8	387.0	759.0
0.2	56.52	Test	35.70	71.50	176.5	250.0
		FEM	49.80	311.0	872.0	1709

experimentally and numerically using the assumption given in Eqs. (6) and (7). In long beams, the results are consistent with each other in the first and second frequencies. As the length of the specimen gets smaller the results differ since the finite element model is not valid for short curved beams. As the specimens get smaller, the member looks like a vibrating straight plate instead of a curved beam. FEM is used for only slightly curved members. Also as the length gets smaller, the mass of the specimen becomes smaller than that of the measurement system. Together with the statements mentioned in the previous paragraph, these effects are decreasing experimental natural frequency values.

Table 3 Natural frequencies, $R = 2.864$ m, $h = 2.2$ mm, $b = 16$ mm

	c (m)	Type	f_1 (Hz)	f_2 (Hz)	f_3 (Hz)	f_4 (Hz)
$L = 0.992$ m $a = h/10$	0.092	Test	1.70	10.00	30.00	60.00
		FEM	1.85	11.46	32.36	63.57
		FEM uncr.	1.86	11.47	32.37	63.58
$L = 0.993$ m $a = h/10$	0.893	Test	1.80	19.00	41.00	62.00
		FEM	1.85	11.44	32.29	63.44
		FEM uncr.	1.86	11.44	32.30	63.45
$L = 0.690$ m $a = h/10$	0.490	Test	3.80	21.00	58.00	100.0
		FEM	3.837	23.85	67.05	131.58
		FEM uncr.	3.838	23.86	67.08	131.61
$L = 0.400$ m $a = h/10$	0.200	Test	11.00	62.00	139.0	272.0
		FEM	11.41	71.28	200.0	391.7
$L = 0.400$ m $a = 2h/10$	0.200	Test	10.00	61.00	135.0	250.0
		FEM	11.40	71.16	199.9	391.0
		FEM uncr.	11.41	71.32	200.0	391.9
$L = 0.300$ m $a = 2h/10$	0.100	Test	20.00	100.0	235.0	500.0
		FEM	20.25	126.8	354.71	696.8
$L = 0.300$ m $a = 3h/10$	0.100	Test	20.00	98.00	210	696.0
		FEM	20.19	126.6	353.5	696.35
		FEM uncr.	20.28	126.9	355.6	696.84

Table 4 Natural frequencies, $R = 1.284$ m, $h = 2.4$ mm, $b = 15$ mm, $L = 0.8$ m, $a = h/10$

c (m)	Type	f_1 (Hz)	f_2 (Hz)	f_3 (Hz)	f_4 (Hz)
0.100	Test	2.30	15.33	42.00	90.00
	FEM	3.12	18.65	53.63	105.96
0.700	Test	2.33	17.00	41.00	91.00
	FEM	3.13	18.68	53.65	105.97
uncracked	FEM	3.14	18.69	53.66	105.97

In Tables 3 and 4, natural frequencies of cracked members are presented and compared with those of uncracked one. Here only single crack case is discussed. The frequencies decrease as the crack depth increases. When the crack is closer to the free end, the frequencies become closer to those of uncracked case. One can see better this behavior in Table 4.

In Tables 5 and 6, the experimental results and comparison of the first five natural frequencies for cracked and uncracked cases are given for two cracks and three cracks, respectively. The locations and depths are arbitrary. Some results are the same up to 2 digits.

Table 5 Natural frequencies, $R = 2.864$ m, $h = 2.2$ mm, $b = 16$ mm, $L = 0.795$ m

c (m)	Depth (mm)	Type	f_1 (Hz)	f_2 (Hz)	f_3 (Hz)	f_4 (Hz)
0.1-0.2	0.24-0.24	Test	2.33	17.33	43.33	90.33
		FEM	2.89	17.93	50.48	99.06
	0.48-0.48	Test	2.33	14.33	41.33	87.33
		FEM	2.88	17.93	50.44	98.97
0.6-0.7	0.24-0.24	Test	2.33	17.33	47.67	89.67
		FEM	2.89	17.94	50.47	99.05
	0.48-0.48	Test	2.33	14.00	47.00	89.66
		FEM	2.89	17.93	50.41	98.90
uncracked		Test	3.00	18.00	50.48	99.08
		FEM	2.89	17.94	50.49	99.10

Table 6 Natural frequencies, $R = 1.284$ m, $h = 2.4$ mm, $b = 15$ mm, $L = 0.8$ m, $c = 0.095, 0.195, 0.295$ m

Depth (mm)	Method	f_1 (Hz)	f_2 (Hz)	f_3 (Hz)	f_4 (Hz)
0.22-0.22-0.22	Test	2.67	17.00	47.67	90.14
	FEM	3.13	18.68	53.64	105.95
0.44-0.44-0.22	Test	2.33	17.00	41.00	90.35
	FEM	3.13	18.67	53.61	105.88
0.66-0.44-0.22	Test	2.33	16.67	41.00	90.25
	FEM	3.12	18.66	53.61	105.90
0.66-0.44-0.44	Test	2.33	17.00	41.50	90.67
	FEM	3.12	18.65	53.58	105.86
0.66-0.66-0.66	Test	2.30	15.33	41.50	91.00
	FEM	3.11	18.64	53.48	105.74
uncracked	Test	2.70	17.40	53.60	96.50
	FEM	3.14	18.69	53.66	106.00

The experimental three crack case (0.095 m, 0.195 m, 0.295 m) is depicted in Figs. 7 and 8 for $L = 0.8$ m, $R = 1.284$ m, $h = 2.4$ mm, $b = 15$ mm. The depths of all cracks are equal, e.g., $a = 0.22$ mm.

The results are good (slightly different) up to the third mode, later there is considerable difference between the frequencies obtained experimentally and numerically. The reason is that both shear deflection and rotatory inertia decrease the natural frequencies. The effect of shear deflection is more important than that of rotatory inertia. The higher are they, the more the natural frequencies are affected (Géradin and Rixen 1997). At higher modes, their effects become more important. In addition to those, transverse and rotatory inertia of the accelerometer are also important so that the natural frequencies obtained experimentally are less than those obtained numerically. Shear is

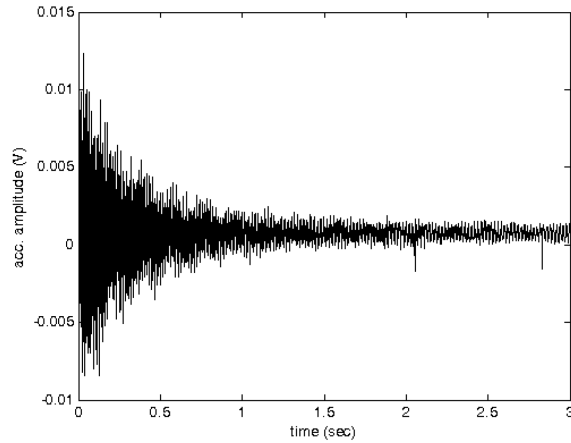


Fig. 7 Acceleration data for three crack case (0.095 m, 0.195 m, 0.295 m), for $L = 0.8$ m, $R = 1.284$ m, $h = 2.4$ mm, $b = 15$ mm

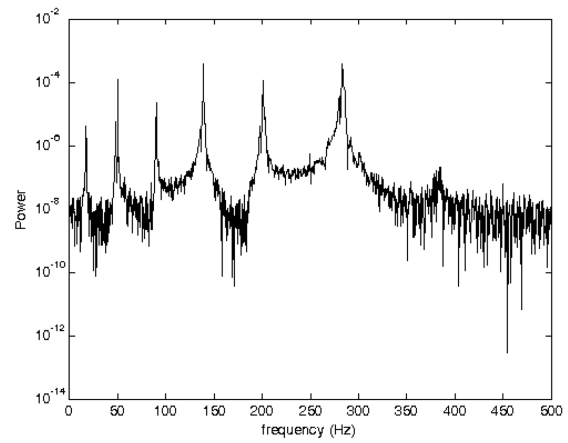


Fig. 8 Spectrum for three crack case (0.095 m, 0.195 m, 0.295 m), for $L = 0.8$ m, $R = 1.284$ m, $h = 2.4$ mm, $b = 15$ mm

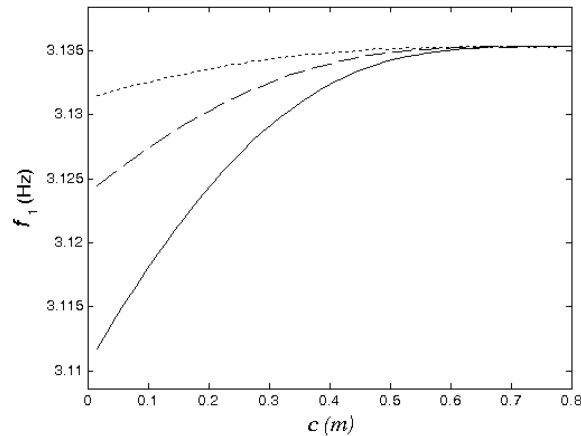


Fig. 9 Variation of the first natural frequency with crack location and depth, $a = h/10$ (...), $a = 2h/10$ (- - -), $a = 3h/10$ (—)

excluded in FEM solution and lumped mass effect is also excluded. Also structural damping and air friction change (decrease) the frequencies and they are not included in FEM. Torsional vibrations are not included in FEM but it has some effect in the measurements. Experimental values are dependent on all of these parameters and properties.

Some analysis can be performed directly using FEM. In Fig. 9, variation of the first natural frequencies are shown for a clamped-free member with $R = 1.284$ m, $L = 0.8$ m, $h = 0.0024$ m, $b = 0.0150$ m. Crack depths are $a = h/10$, $a = 2h/10$ and $a = 3h/10$. When the crack is close to the clamped end, it has higher effect on the frequencies. As the crack is close to the free end, the frequencies become closer to the uncracked case. Increasing the depth decreases the frequencies further. Comparing with Table 4, at $c = 0.1$ and 0.7 m, the experimental values are 2.30 and 2.33 Hz, respectively. For $c = 0.1$ m, the difference is 27% and for $c = 0.7$, the difference is 25% in the first

mode between experimental and numerical results. In the second mode, for $c = 0.1$ m, the difference is 18%, for $c = 0.7$ m, the difference is 9%. In the third mode, for $c = 0.1$ m, the difference is 22%, for $c = 0.7$ m, the difference is 24%. In the fourth mode, for $c = 0.1$ m, the difference is 15%, for $c = 0.7$ m, the difference is 14%.

The second, third and fourth mode variations are shown in Figs. 10-12. Similar conclusions can be drawn. The crack at the point of maximum displacement does not affect the frequencies too much as seen in the figures (Krawczuk and Ostachowicz 1997). If the moment is a maximum at some other locations (e.g., nodal points and clamped end), the frequencies will be very much lower than those of the uncracked one because of large moment due to higher stress concentration (Krawczuk and Ostachowicz 1997, Öz and Daş 2006). The greatest effect is at the locations close to the clamped end. In the second mode, at $c \cong 0.43$, in the third mode at $c \cong 0.25$ and 0.57 m, in the fourth mode at $c \cong 0.17$, 0.40 , and 0.63 m, the frequencies decrease too much e.g., these points are

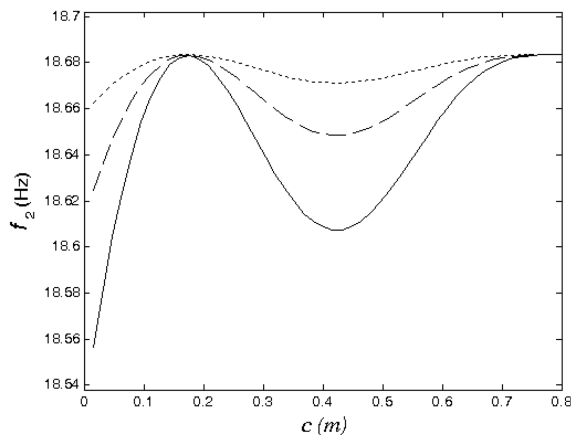


Fig. 10 Variation of the second natural frequency with crack location and depth $a = h/10$ (....), $a = 2h/10$ (- - -), $a = 3h/10$ (—)

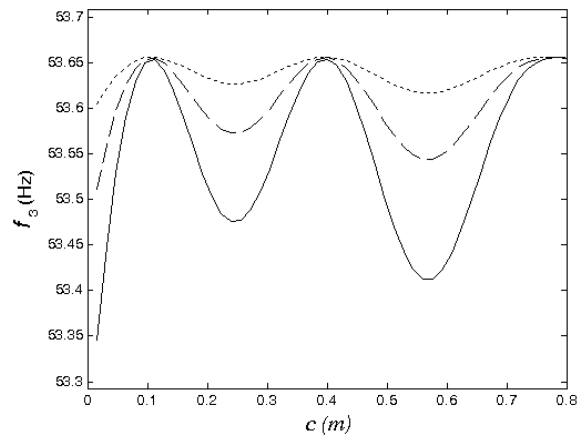


Fig. 11 Variation of the third natural frequency with crack location and depth $a = h/10$ (....), $a = 2h/10$ (- - -), $a = 3h/10$ (—)

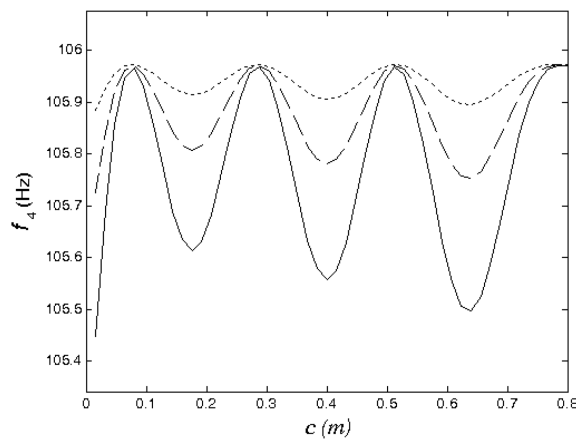


Fig. 12 Variation of the fourth natural frequency with crack location and depth $a = h/10$ (....), $a = 2h/10$ (- - -), $a = 3h/10$ (—)

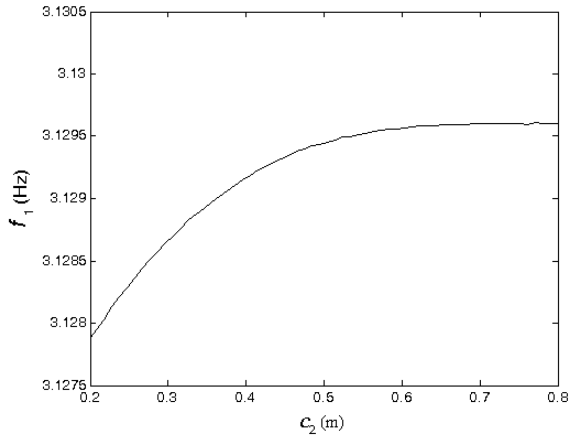


Fig. 13 Variation of the first natural frequency with crack locations at $c_1 = 0.1L$, $c_2 = 0.2L-L$, depths $a_1 = a_2 = h/10$

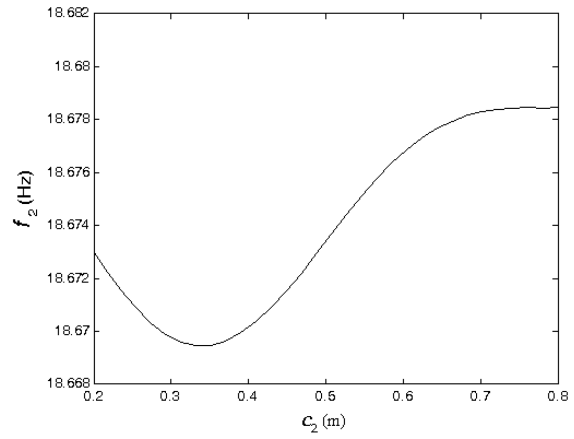


Fig. 14 Variation of the second natural frequency with crack locations at $c_1 = 0.1L$, $c_2 = 0.2L-L$, depths $a_1 = a_2 = h/10$

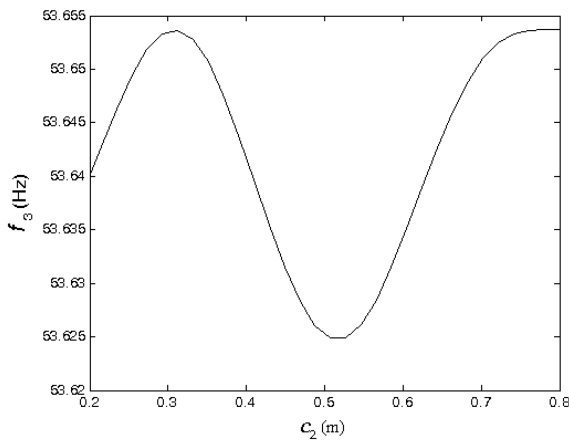


Fig. 15 Variation of the third natural frequency with crack locations at $c_1 = 0.1L$, $c_2 = 0.2L-L$, depths $a_1 = a_2 = h/10$

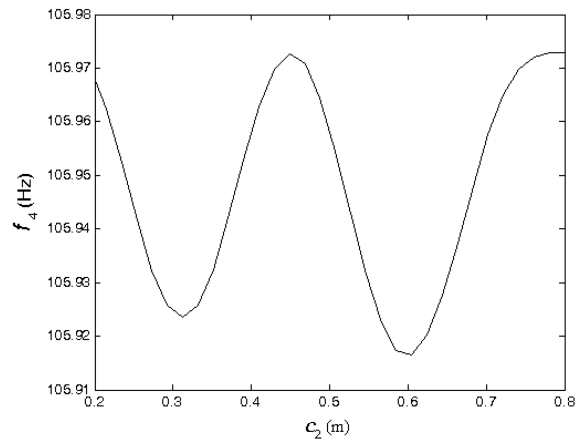


Fig. 16 Variation of the fourth natural frequency with crack locations at $c_1 = 0.1L$, $c_2 = 0.2L-L$, depths $a_1 = a_2 = 0.00022$ m, $h/10$

nodal points. The decrease in natural frequencies was emphasized by Öz and Daş (2006) numerically using the relation presented in the current study and also by Cerri and Ruta (2004), Viola *et al.* (2005) and Cerri *et al.* (2008) in which springs were used to model the crack and by Yaghin and Hesari (2008) who mentioned the effect of local stiffness difference in a simulation study of a damaged arch dam.

Let's consider two crack case and discuss the natural frequency variation numerically with the crack location and depth. For the member with $R = 1.284$ m, $L = 0.8$ m, $h = 0.0024$ m, $b = 0.0150$ m, the depths of two cracks are the same, $a = h/10$, but the first one is at $0.1L$, the second crack is assumed to be between $0.2L$ and L , The variation of natural frequencies are presented in Figs. 13-16. When the crack is around the nodal points, the frequencies decrease too much. Since some nodal points are before $0.2L$, they are not seen in the figures.

Similar analysis can be performed for three crack cases, no figures will be given here but the data can be observed in Table 6.

4. Conclusions

The subject of the paper is the in-plane dynamics of slightly curved cracked circular beams. The beam is clamped at one end and has a transverse open crack or cracks on it. The cracks do not propagate during vibrations. An approach proposed for straight beams is used in calculating the effect of cracks on the natural frequencies of a slightly curved beam. In the numerical solution Rayleigh type beam is considered. Bending, extension and rotation effects are included in the vibrations but shear effect is excluded. Thin cracks are opened by a hand saw at different locations. Acceleration data is recorded and processed to obtain the frequencies. Experimental and finite element solutions are compared to examine the proposed approach for different crack locations, numbers of cracks and depths. Increasing the crack depth decreases the frequencies. As the number of crack increases, the frequencies decrease fast. When the crack is opened around nodes, the natural frequencies are affected too much due to larger moments. Its effect is negligible when it is at the location of maximum displacements. The greatest effect is at the locations close to the clamped end. Since the moment is zero at the free end, there is no effect due to the crack. The results of FEM and those obtained by experimentation show better consistency for longer beams. When the length of the beam becomes shorter, e.g., it becomes a plate instead of a beam; the values become more different since the FEM becomes invalid. Also the weight of the measurement system (mass and rotatory inertia) affects the frequencies. Its effect is more important in shorter beams. The shear effect in the curved member is also important since it is excluded in FEM. The reasons for difference between experimentally and numerically obtained frequencies can be summarized as follows: the validity of flexural rigidity equation obtained for straight beams and its usage for a slightly curved beam especially for multi crack case, mass and rotatory inertia of the measurement system, degree of validity of FEM for shorter beams, shear effect, structural damping, air friction, torsional vibration behavior in longer beam samples. This study can give information for the need of equations to be used for curved beams to improve results.

References

- Alves, S.W. and Hall, J.F. (2006), "System identification of a concrete arch dam and calibration of its finite element model", *Earthq. Eng. Struct. Dyn.*, **35**(11), 1321-1337.
- Andrasic, C.P. and Parker, A.P. (1980), "Weight functions for cracked, curved beams", Eds. Owen, D.R.F., Luxmoore, A.R., *Numerical Methods in Fracture Mechanics*, Swansea, 67-82.
- Bovsunovsky, A.P. and Matveev, V.V. (2000), "Analytical approach to the determination of dynamic characteristics of a beam with a closing crack", *J. Sound Vib.*, **235**(3), 415-434.
- Cerri, M.N., Dilena, M. and Ruta, G.C. (2008), "Vibration and damage detection in undamaged and cracked circular arches: Experimental and analytical results", *J. Sound Vib.*, **314**, 83-94.
- Cerri, M.N. and Ruta, G.C. (2004), "Detection of localized damage in plane circular arches by frequency data", *J. Sound Vib.*, **270**, 39-59.
- Chidamparam, P. and Leissa, A.W. (1995), "Influence of centerline extensibility on the in-plane free vibrations of loaded circular arches", *J. Sound Vib.*, **183**(5), 779-795.

- Chondros, T.G., Dimarogonas, A.D. and Yao, J. (1998), "A continuous cracked beam vibration theory", *J. Sound Vib.*, **215**(1), 17-34.
- De Rosa, M.A. and Franciosi, C. (2000), "Exact and approximate dynamic analysis of circular arches using DQM", *Int. J. Solids Struct.*, **37**, 1103-1117.
- Fernández-Sáez, J., Rubio, L. and Navarro, C. (1999), "Approximate calculation of the fundamental frequency for bending vibrations of cracked beams", *J. Sound Vib.*, **225**(2), 345-352.
- Ibrahimbegovic, A. (1995), "On finite element implementation of geometrically nonlinear Reissner's beam theory: three dimensional curved beam elements", *Comput. Meth. Appl. Mech. Eng.*, **122**, 11-26.
- Kapp, J.A., Newman, Jr, J.C. and Underwood, J.H. (1980), "A wide range stress intensity factor expression for the C-shaped specimen", *J. Test Eval., JTEVA*, **8**(6), 314-317.
- Kang, K. and Bert, C.W. (1997), "Flexural-torsional buckling analysis of arches with warping using DQM", *Eng. Struct.*, **19**(3), 247-254.
- Khan, A.K. and Pise, P.J. (1997), "Dynamic behaviour of curved piles", *Comput. Struct.*, **65**(6), 795-807.
- Khiem, N.T. and Lien, T.V. (2001), "A simplified method for natural frequency analysis of a multiple cracked beam", *J. Sound Vib.*, **245**(4), 737-751.
- Kisa, M., Brandon, J. and Topçu, M. (1998), "Free vibration analysis of cracked beams by a combination of finite elements and component mode synthesis methods", *Comput. Struct.*, **67**, 215-223.
- Krawczuk, M. and Ostachowicz, W.M. (1997), "Natural vibrations of a clamped-clamped arch with an open transverse crack", *J. Vib. Acoust.*, **119**, 145-151.
- Krishnan, A., Dharmaraj, S. and Suresh, Y.J. (1995), "Free vibration studies of arches", *J. Sound Vib.*, **186**(5), 856-863.
- Krishnan, A. and Suresh, Y.J. (1998), "A simple cubic linear element for static and free vibration analyses of curved beams", *Comput. Struct.*, **68**, 473-489.
- Love, A.E.H. (1944), *Treatise on the Mathematical Theory of Elasticity*, 4th Edition, Dover, NY.
- Müller, W.H., Herrmann, G. and Gao, H. (1993), "A note on curved cracked beams", *Int. J. Solids Struct.*, **30**(11), 1527-1532.
- Nobile, L. (2000), "Mixed mode crack initiation and direction in beams with edge crack", *Theoret. Appl. Fracture Mech.*, **33**, 107-116.
- Nobile, L. (2001), "Mixed mode crack growth in curved beams with radial edge crack", *Theoret. Appl. Fract. Mech.*, **36**, 61-72.
- Oh, S.J., Lee, B.K. and Lee, I.W. (2000), "Free vibrations of non-circular arches with non-uniform cross-section", *Int. J. Solids Struct.*, **37**, 4871-4891.
- Öz, H.R. and Dağ, M.T. (2006), "In-plane vibrations of circular curved beams with a transverse open crack", *Mathem. Comput. Appl.*, **11**(1), 1-10.
- Öz, H.R. and Özkaya, E. (2005), "Three-to-one internal resonances in a curved beam resting on an elastic foundation", *Int. J. Appl. Mech. Eng.*, **10**(4) 667-678.
- Öz, H.R., Pakdemirli, M., Özkaya, E. and Yılmaz, M. (1998), "Nonlinear vibrations of a slightly curved beam resting on a nonlinear elastic foundation", *J. Sound Vib.*, **212**(2) 295-309.
- Öz, H.R. and Pakdemirli, M. (2006), "Two-to-one internal resonances in a shallow curved beam resting on an elastic foundation", *Acta Mech.*, DOI 10.1007/s00707-006-0352-5.
- Özyiğit, H.A., Öz, H.R. and Tekelioğlu, M. (2004), "Linear forced in-plane and out-of-plane vibrations of frames having a curved member", *Mathem. Comput. Appl.*, **9**, 371-380.
- Petyt, M. (1990), *Introduction to Finite Element Vibration Analysis*, Cambridge University Press, U.K.
- Raveendranath, P., Singh, G. and Pradhan, B. (2000), "Free vibration of arches using a curved beam element based on a coupled polynomial displacement field", *Comput. Struct.*, **78**, 583-590.
- Saavedra, P.N. and Cuitino, L.A. (2001), "Crack detection and vibration behavior of cracked beams", *Comput. Struct.*, **79**, 1451-1459.
- Tong, X., Mrad, N. and Tabarrok, B. (1998), "In-plane vibration of circular arches with variable cross-sections", *J. Sound Vib.*, **212**(1), 121-140.
- Tracy, P.G. (1975), "Analysis of a radial crack in a circular ring segment", *Eng. Fract. Mech.*, **7**, 253-260.
- Tüfekçi, E. and Arpacı, A. (1998), "Exact solution of in-plane vibrations of circular arches with account taken of axial extension, transverse shear and rotatory inertia effects", *J. Sound Vib.*, **209**(5), 845-856.

- Viola, E., Artioli, E. and Dilena, M. (2005), "Analytical and differential quadrature results for vibration analysis of damaged circular arches", *J. Sound Vib.*, **288**, 887-906.
- Viola, E., Dilena, M. and Tornabene, F. (2007), "Analytical and numerical results for vibration analysis of multi-stepped and multi-damaged circular arches", *J. Sound Vib.*, **299**, 143-163.
- Viola, E. and Tornabene, F. (2005), "Vibration analysis of damaged circular arches with varying cross-section", *Tech Science Press, SID*, **1**(2), 155-169.
- Walsh, S.J. and White, R.G. (1999), "Mobility of a semi-infinite beam with constant curvature", *J. Sound Vib.*, **221**(5), 887-902.
- Yaghin, M.A.L. and Hesari, M.A. (2008), "Using wavelet analysis in crack detection at the arch concrete dam under frequency analysis with FEM", *J. Wavel. Theor. Appl.*, **2**(1), 61-81.
- Yang, X.F., Swamidass, A.S.J. and Seshadri, R. (2001), "Crack identification in vibrating beams using the energy method", *J. Sound Vib.*, **244**(2), 339-357.
- Zheng, D.Y. and Kessissoglou, N.J. (2004), "Free vibration analysis of a cracked beam by finite element method", *J. Sound Vib.*, **273**, 457-475.
- Geradin, M. and Rixen, D. (1997), *Mechanical Vibrations, Theory and Application to Structural Dynamics*, 2nd Edition, John Wiley & Sons Ltd., Eastbourne, GB.

